1521-009X/42/3/431–440$25.00
DRUG METABOLISM AND DISPOSITION

http://dx.doi.org/10.1124/dmd.113.055434
Drug Metab Dispos 42:431–440, March 2014

Biodistribution and Metabolism Studies of Lipid Nanoparticle–Formulated Internally [^{3}H]-Labeled siRNA in Mice[S]

Jesper Christensen, Karine Litherland, Thomas Faller, Esther van de Kerkhof, François Natt, Jürg Hunziker, Julien Boos, Iwan Beuvink, Keith Bowman, Jeremy Baryza, Mike Beverly, Chandra Vargeese, Olivier Heudi, Markus Stoeckli, Joel Krauser, and Piet Swart

Drug Metabolism and Pharmacokinetics (J.C., K.L., T.F., E.v.d.K., O.H., J.K., P.S.), Analytical Sciences (M.S.), and Biologics Center (F.N., J.H., J.Bo., I.B.), Novartis Pharma AG, Novartis Institutes for Biomedical Research, Basel, Switzerland; and Biologics Center, Novartis Pharma AG, Novartis Institutes for Biomedical Research, Cambridge, Massachusetts (K.B., J.B., M.B., C.V.)

Received October 14, 2013; accepted January 3, 2014

ABSTRACT

Absorption, distribution, metabolism, and excretion properties of a small interfering RNA (siRNA) formulated in a lipid nanoparticle (LNP) vehicle were determined in male CD-1 mice following a single intravenous administration of LNP-formulated [^{3}H]-SSB siRNA, at a target dose of 2.5 mg/kg. Tissue distribution of the [^{3}H]-SSB siRNA was determined using quantitative whole-body autoradiography, and the biostability was determined by both liquid chromatography mass spectrometry (LC-MS) with radiodetection and reverse-transcriptase polymerase chain reaction techniques. Furthermore, the pharmacokinetics and distribution of the cationic lipid (one of the main excipients of the LNP vehicle) were investigated by LC-MS and matrix-assisted laser desorption ionization mass spectrometry imaging techniques, respectively. Following i.v. administration of [^{3}H]-SSB siRNA in the LNP vehicle, the concentration of parent guide strand could be determined up to 168 hours p.d. (post dose), which was ascribed to the use of the vehicle. This was significantly longer than what was observed after i.v. administration of the unformulated [^{3}H]-SSB siRNA, where no intact parent guide strand could be observed 5 minutes post dosing. The disposition of the siRNA was determined by the pharmacokinetics of the formulated LNP vehicle itself. In this study, the radioactivity was widely distributed throughout the body, and the total radioactivity concentration was determined in selected tissues. The highest concentrations of radioactivity were found in the spleen, liver, esophagus, stomach, adrenal, and seminal vesicle wall. In conclusion, the LNP vehicle was found to drive the kinetics and biodistribution of the SSB siRNA. The renal clearance was significantly reduced and its exposure in plasma significantly increased compared with the unformulated [^{3}H]-SSB siRNA.

Introduction

RNA interference (RNAi) stands out from traditional pharmaceutical drug research, which typically focuses on interactions of small molecules with proteins. RNAi-designed drugs inhibit or break down the messenger RNA of the protein of interest. Theoretically, RNAi can silence or slow down the production of any protein. The RNAi pathway is initiated by double-stranded 21-23mer oligonucleotides, also known as small interfering RNAs (siRNAs). They are highly vulnerable toward nuclease activities leading to very short half-lives and a rapid renal clearance. To some extent, this can be circumvented by chemical modifications of the siRNAs. However, chemical stabilization of the siRNA alone often results in renal clearance of intact siRNA without degradation (Behlke, 2008). In addition, siRNAs can also have specificity issues, which can result in off-target silencing or stimulation of the innate immune system. As such, systemic delivery of unformulated siRNA seems more unlikely to be successful (Christensen et al., 2013). For future applications of siRNAs as therapeutics, delivery systems are anticipated to hold the key to their success. Today, the delivery of siRNAs remains one of the main hurdles for their development as therapeutics (Burnett et al., 2011; Rettig and Behlke, 2012).

However, a variety of delivery systems using conjugated or complexation approaches have been successfully applied to improve siRNA targeting. For some of these delivery systems, the biodistribution has been studied after systemic administration to mice, using radioactive isotopes. Typically, the siRNA has been labeled (Bartlett et al., 2007; Sonoke et al., 2008; Gao et al., 2009; Malek et al., 2009; Merkel et al., 2009a,b; Hatanaka et al., 2010; Mudd et al., 2010), but the vehicle has also been reported as the labeled component (Merkel et al., 2009b; Hatanaka et al., 2010; Mudd et al., 2010).

The influences of the applied labeling methods on the pharmacokinetic behavior of the siRNAs studied are often assumed to not alter

dx.doi.org/10.1124/dmd.113.055434.
[S]This article has supplemental material available at dmd.aspetjournals.org.

ABBREVIATIONS: ADME, absorption, distribution, metabolism, and excretion; AUC∞, area under the curve infinity; AUC_{last}, area under the curve until last time point; DLin-KC2-DMA, 2,2-dilinoleyl-4-(2-dimethylaminoethyl)-[1,3]-dioxolane; HPLC, high-performance liquid chromatography; LC-MS, liquid chromatography mass spectrometry; LNP, lipid nanoparticle; LSC, liquid scintillation counting; MALDI-MSI, matrix-assisted laser desorption ionization mass spectrometry imaging; PBS, phosphate-buffered saline; PCR, polymerase chain reaction; p.d., post dose; PK, pharmacokinetic; QWBA, quantitative whole-body autoradiography; RA, radioactivity; RES, reticuloendothelial system; RNAi, RNA interference; RT-qPCR, quantitative reverse-transcriptase polymerase chain reaction; SEC, size exclusion chromatography; siRNA, short interfering RNA; SPE, solid phase extraction; SSB, Sjögren syndrome antigen B.

the reactivity or metabolism of the molecule. Nevertheless, the choice of labeling approach has previously been shown to influence the pharmacokinetic behavior of large molecules, such as for siRNAs (Christensen et al., 2013). There are several radiolabels that have been used for this approach: ^{3}H, ^{18}F, ^{32}P, ^{64}Cu, ^{111}In. The beauty of replacing a ^{1}H (or ^{12}C) atom by its radioactive ^{3}H (or ^{14}C) is that the structure as such is not altered and has the least impact on the pharmacokinetic (PK). For our work, we chose the SSB siRNA which targets the ubiquitous gene Sjögren syndrome antigen B (SSB). Therefore, we applied a single internal [^{3}H]-radiolabeling procedure, in which the full-length oligonucleotides were radiolabeled by Br/^{3}H exchange (Christensen et al., 2012). This labeling method avoids chemical modification of the siRNA by placing the tritium atom in a chemically stable and predetermined internal position. The cationic lipid DLin-KC2-DMA was not labeled, but its concentrations were followed by LC-MS analysis.

For the concentration determination of free versus encapsulated radioactivity in blood/plasma, an approach using the combination of agarose gel electrophoresis and radiometry was developed and applied for plasma. The hypothesis behind this approach was that free oligonucleotides (negatively charged) would be separated from encapsulated oligonucleotides by moving toward the positive pole ("end section" of the gel lane), thereby leaving the encapsulated oligonucleotides in the well. The separated free and encapsulated oligonucleotides could then be isolated and measured by radiometry.

For the distribution part of the study, quantitative whole-body autoradiography (QWBA) and matrix-assisted laser desorption ionization mass spectrometry imaging (MALDI-MSI) techniques were applied. QWBA allows measurement of the radiolabeled siRNA, and MALDI-MSI allows measurement of the cationic lipid [one of the main excipients of the lipid nanoparticle (LNP) vehicle]. The combination of these two techniques provides a strong indication of the fate of the siRNA/LNP complex (cationic lipid analyte as surrogate). As an alternative to QWBA (which requires radiolabeled siRNA), a whole-body scanning polymerase chain reaction (PCR) technique to study the biodistribution of oligonucleotides was recently reported (Boos et al., 2013). Here, we aimed for performing an in vivo experiment and followed PK, distribution, metabolism, and mass balance combining the different methods to assess the absorption, distribution, metabolism, and excretion (ADME) properties of the [^{3}H]-SSB siRNA formulated in an LNP vehicle after intravenous administration to CD-1 mice.

Materials and Methods

Test Compound and Radiolabeling of siRNA

The siRNA was internally labeled with tritium following procedures previously described (Christensen et al., 2012). The 21mer double-stranded sequences were as follows: 5′-UuAcAU**u$_7$**AAAGUCUGUUGUuu-3′ and 5′-AcAAcAGAcuuuAAuGuAAuu-3′ for the guide and passenger strands, respectively. The siRNA was modified via selected incorporation of 2′-O-methyl pyrimidines (u = 2′OMe uridine and c = 2′OMe cytidine) throughout the sequences. The siRNA was uniquely ^{3}H-radiolabeled in the guide strand. The tritium atom was incorporated into the chemically stable C5 position of the predetermined 2′-O-methyluridine (bold typed). The radiochemical purity was 73% by ion pair reversed phase (RP) high-performance liquid chromatography (HPLC).

LNP Formulation

The radioactive dosing solution of LNP-formulated SSB siRNA in phosphate-buffered saline (PBS) buffer was prepared as follows: the lipid constituents were 2,2-dilinoleyl-4-(2-dimethylaminoethyl)-[1,3]-dioxolane (DLin-KC2-DMA, cationic lipid), cholesterol (neutral lipid), dipalmitoylphosphatidylcholine (DPPC, helper lipid for nanoparticle stabilization), and N-[(methoxy poly(ethylene glycol)$_{2000}$)carbamoyl]-1,2-dimyristyloxlpropyl-3-amine (PEG-C-DMA lipid) used at a molar ratio of 57.1:34.3:7.1:1.4 as described by Semple et al. (2010). Briefly, the siRNA was diluted and adjusted to a concentration of about 0.9 mg/ml with buffer, containing 25 mM sodium citrate and 100 mM NaCl (pH adjusted to 5.0 with 2 N HCl). The siRNA was mixed through a tee with the lipids dissolved in ethanol. During the mixing, the siRNA-LNP are being formed spontaneously. The mixture was dialyzed and concentrated against pH using an ultra-filtration system. The purified sample was heated to 65°C for 15 minutes and the filter sterilized using a 0.2 μm filter device (polyethersulfone [PES] membrane; Millipore, Merck KGaA, Darmstadt, Germany). The degree of encapsulation of siRNA in the LNP formulation was determined to be 88.3%, by size exclusion chromatography (size exclusion chromatography [SEC]-HPLC-UV). In this assay, free siRNA (nonformulated siRNA, 5 nm) eluted after the liposomes (50–200 nm). For measurement of total siRNA, the surfactant (triton) was added to disrupt the LNP formulation. Encapsulation degree was calculated as follows: [(total siRNA – free siRNA) / total siRNA] × 100%. The siRNA concentration in the LNP formulation was determined to 0.40 mg/ml by SEC-HPLC-UV linear regression method (calibration curve constituted from six dilutions of siRNA reference substance, $R^2 = 0.9999$). The particle size (using photon correlation spectroscopy) of the LNP formulation was measured (129 nm) using a Delsa Nano C particle size instrument from Beckman Coulter (Pasadena, CA).

Due to a limited amount of the radioactive LNP-formulated siRNA available, selected mice were dosed with a nonradioactive LNP formulation. Therefore, a nonradioactive dosing solution of LNP-formulated SSB siRNA was also produced in the same manner with the following specifications: encapsulation degree 91.0%, siRNA concentration 0.78 mg/ml, cationic lipid concentration 3.32 mg/ml, and particle size 141 nm.

In Vivo Experiments

The animal studies were approved by the Animal Care and Use Committees of the Kanton Basel, Switzerland. Male albino CD-1 mice (Charles River France, 31–34 g, 8–10 weeks) received an intravenous bolus injection in the vena saphena of either 2.5 mg/kg radioactive or 2.5 mg/kg nonradioactive LNP-formulated SSB siRNA in PBS buffer under a light inhalation anesthesia by isoflurane. The dose volumes were 6.3 and 3.2 ml/kg (radioactive and nonradioactive, respectively), and the total amount of radioactivity administered was 17–19 MBq/kg. The specific radioactivity of the LNP-formulated [^{3}H]-SSB siRNA was 7.27 MBq/mg.

Due to the limited amount of radioactive LNP formulation available, selected mice were dosed with a nonradioactive LNP formulation, allowing a good characterization of the pharmacokinetics of the parent compound and the cationic lipid DLin-KC2-DMA in the LNP vehicle. After dosing, blood was collected from either the vena saphena (opposite leg than used for dosing) or the vena cava (for endpoints) in EDTA containing tubes at 0.083, 1, 2, 6, 24, 48, 72, 168, 336, 504, and 672 hours post dose (mice dosed with the nonradioactive formulation are underscored). At each endpoint, an aliquot of the blood was processed immediately to plasma by centrifugation at 3000*g* for 10 minutes at 4°C. A small aliquot was taken for total radioactivity detection, and the remainder of the material was snap frozen and stored at −80°C until further analysis.

Selected animals were housed in metabolic cages, at various intervals (no longer than 1 week) over a 3-week period, for urine and feces collection, allowing determination of the route of excretion and the mass balance. QWBA was performed at 1, 48, and 168 hours. The use of animals was minimized during these studies (14 mice were dosed in total, 5 of which were nonradioactively dosed), i.e., selected mice contributed to at least two types of experiments, allowing a good characterization of its PK, mass balance, routes of excretion, metabolism profiles, and distribution.

Analytical Methods

Radiometric Analysis. Radioactive signals in the different matrices were quantified by liquid scintillation counting (LSC), using Liquid Scintillation Systems 2500 TR from Packard Instrument Co. (Meriden, CT). For quench correction, an external standard ratio method was used. Quench correction curves were established by means of sealed standards (Packard). Background

values were prepared for each batch of samples according to the respective matrix. The limit of detection was defined as 1.8 times the background value. All determinations of radioactivity were conducted in weighed samples. To determine possible formation of tritiated water, samples were analyzed twice: direct measurements of radioactivity and after drying of the sample (at 37°C for at least 12 hours). Dried or nondried plasma and urine were mixed with scintillation cocktail directly, whereas whole-blood and feces samples were solubilized before radioactivity analysis. Measured radioactivity for blood, plasma, and tissues was converted into concentrations (mole equivalents per volume or gram) considering the specific radioactivity and assuming a matrix density of 1 g/ml.

Quantitative Whole-Body Autoradiography

Mice were sacrificed by deep isoflurane inhalation. After deep anesthesia, blood for radioactivity determination by LSC was collected by the vena saphena (the leg other than the one used for dosing). The animals were then submerged in n-hexane/dry ice at −70°C for approximately 30 minutes. The carcasses were stored at −18°C and all subsequent procedures were performed at temperatures below −20°C to minimize diffusion of radiolabeled materials into thawed tissues. Sections were prepared as follows: in brief, 40 μm thick, lengthwise, dehydrated, whole-body sections were prepared and exposed to Fuji BAS III imaging plates (Fuji Photo Film Co., Ltd., Tokyo, Japan) in a lead-shielded box at room temperature for 2 weeks, and then scanned in a Fuji BAS 5000 phosphor imager (Fuji Photo Film) at a 50 μm scanning step. The concentrations of total radiolabeled components in the tissues were determined by comparative densitometry and digital analysis of the autoradiogram; blood samples of known concentrations of total radiolabeled components processed under the same conditions were used as calibrators.

MALDI-MS Imaging

For mass spectrometric imaging, whole-body sections were lyophilized at −40°C overnight and mounted on metal plates. The sections were coated with α cyano-4-hydroxycinnamic acid matrix at a concentration of 10 mg/ml in 50% acetonitrile and 0.1% aqueous trifluoroacetic acid (v/v) containing 2 nmol/μl of imatinib. The matrix deposition was performed on an in-house built spraying device based on an X-Y-Z liquid handling robot (Cavro, Sunnyvale, CA), depositing 80 ml of matrix solution over an area of 400 cm^2 in 21 cycles during 20 minutes. Mass spectrometric images were acquired on the FlashQuant system (AB SCIEX, Toronto, Canada) with a spatial resolution of 0.5 mm, observing a transition from *m/z* 642.8 to 116.2. The images were normalized with the MS signal response from imatinib applied to the section during matrix deposition.

Quantification of Parent Guide and Passenger Strands by Reverse-Transcriptase Polymerase Chain Reaction

The guide and passenger strands of the SSB siRNA were quantified in plasma by quantitative reverse-transcriptase polymerase chain reaction (RT-qPCR). The matrix was diluted such that the siRNA levels were within the linear range of the standard curve used. The nucleic acid molecules were amplified using a 7900HT Fast Real-Time PCR system (Applied Biosystems, Toronto, Canada), and simultaneously quantified using a standard curve of the target.

Quantification of Cationic Lipid by LC-MS

The vehicle containing the cationic lipid DLin-KC2-DMA was quantified in plasma following protein precipitation using standard LC-MS methods. Five-microliter samples were injected on a reverse-phase C18 column (Supelco Ascentis Express, Sigma-Aldrich, Bellefonte, Pennsylvania; 50 × 2.1 mm; 2.7-μm particles) equipped with a guard column (Supelco Ascentis Express; 5 × 2.1 mm; 2.7-μm particles). The column was maintained at 50°C, and the flow rate on the column was 0.85 ml/min (eluent A: water containing 0.1% formic acid; eluent B: ethanol). The following gradient was applied: 30% B for 0.5′ → 136% B/min → 98% B after 0.5′ → 98% B for 2′ → −680% B/min → 30% B after 0.1′→ 30% B for 0.9′. Before MS, the effluent was mixed with 0.40 ml/min mobile phase B. Mass measurements were made online using an API4000 mass spectrometer (Applied Biosystems). The mass spectrometer was set to scan in electrospray ionization (ESI) positive mode with the following specifications: spray voltage 5.5 kV, curtain gas flow 20 psi, source temperature 650°C, dwell time 80 ms, entrance potential of 10 V, collision energy 39.0 V, collision cell exit potential 8 V, and declustering potential 96 V.

Determination of Free Radioactivity by Gel Electrophoresis and Radiometry

Plasma samples (~20 μl) containing DNA loading dye (Fermentas, VWR International, Darmstadt, Germany) were subjected to agarose (2% in Tris/borate/EDTA buffer, pH 8) gel electrophoresis and stained for nucleic acid using SYBR gold dye (in dimethylsulfoxide; Invitrogen, Carlsbad, CA). Triton (10%–20%) was added to control samples. The gels were developed at 70 V in Tris/borate/EDTA buffer, and the siRNA was visualized under a UV lamp (λ = 254 nm). Each gel lane was cut into three sections (i.e., well, middle, and end). The sections were dissolved in dimethylsulfoxide (2 ml/g gel) and placed in an oven overnight at 70°C (cap of scintillation vial slightly loose). Irga-safe plus scintillation cocktail (Zinsser Analytic, Frankfurt, Germany, flash point >120°C) was added to a total volume of 19 ml, shaken, and measured immediately by radiometry (LSC). The method was developed with mouse blood and plasma samples (mixed gender; SeraLab, Haywards Heath, United Kingdom) spiked with [^{3}H]-SSB siRNA in 0.9% NaCl, at a concentration of 4 μM (36 KBq/ml). A PBS control sample was used. The method was validated by spiking plasma with the dosing solution of LNP-formulated [^{3}H]-SSB siRNA, at a concentration of 4 μM (40 KBq/ml).

Sample Preparation of Plasma for Metabolite Profiling

For metabolite profiling of plasma, the oligonucleotides were extracted and isolated by the use of Clarity OTX, weak anion exchange solid phase extraction cartridges from Phenomenex (WAX-SPE; Torrance, CA), according to the manufacturer's instructions. In addition, 0.1% triton was added to the lysis-loading buffer, to disrupt the LNP formulation. Extraction recoveries of radioactivity of the plasma extraction procedure were all above 85%.

HPLC-MS-RA metabolite identification of oligonucleotide metabolites

Selected plasma samples were analyzed for metabolite identification purposes by ion pairing reverse-phase HPLC-MS-radioactivity (RA). Separation was accomplished using an HPLC system from Agilent Technologies (Santa Clara, CA), 1100 Series, equipped with a binary capillary pump, including a degasser, an autosampler, a column oven, and a diode array detector. The operating software monitoring the HPLC system was LC/MSD Chemstation version B.04.02 (Agilent Technologies). Ten-microliter samples were injected on a reverse-phase C18 column (Waters XBridge Shield; 150 × 2.1 mm; 3.5-μm particles) equipped with a guard column (Waters XBridge; 10 × 2.1 mm; 3.5-μm particles; Waters, Milford, MA). The column was maintained at 70°C (denaturing conditions), and the flow rate on the column was 0.25 ml/min. Eluent A was made up of 1.6 mM triethylamine and 100 mM hexafluoroisopropanol (pH ~7.5), and eluent B was made up of 1.6 mM triethylamine and 100 mM hexafluoroisopropanol in 40% methanol. The following gradient was applied: 0% B for 10′ → 2.5% B/min → 50% B after 20′ → 450% B/min → 95% B after 0.1′ → 95% B for 4.9′ → -950% B/min → 0% B after 0.1′→ 0% B for 4.9′. After elution from the column, the effluent was split. Approximately 20 μl was directed to the MS, while the remaining flow was monitored by a diode array detector (DAD) at λ = 260 nm and collected into 96-well Luma plates using a fraction collector (Gilson FC204, 4.2 seconds fraction size, collect from 0 to 27 minutes; Gilson, Middleton, WI). To help with the fraction collection, a make-up flow composed of mobile phase B was used (Jasco pump, PU-980, 0.25 ml/min; Jasco UK, Great Dunmow, UK). The plates were dried using a speed vac (AES2010; Savant, ThermoFisher, Bremen, Germany) and counted (up to 60 minutes per well, depending on the level of radioactivity) on a Packard TopCount instrument (PerkinElmer, Waltham, MA). Mass measurements were made online using an LTQ-Orbitrap XL mass spectrometer (Thermo Fisher Scientific, Waltham, MA) operating under Xcalibur, version 2.0 for instrument control, data acquisition, and data processing. From 0 to 40 minutes, the mass spectrometer was set to scan in ESI negative mode with resolution set at 30,000 and an *m/z* window from 400 to 2000. Mass spectra were obtained using a spray voltage of 3.6 kV, a sheath gas flow of 16

(arbitrary flow rate), a source temperature of 275°C, and a capillary and tube lens voltage of −53 and −94.3 V, respectively.

Pharmacokinetic Analysis

Pharmacokinetic parameters and QWBA data were calculated using Phoenix WinNonlin software (version 6.1.0.173; Pharsight Corp., Mountain View, CA). The pharmacokinetic estimations were based on a noncompartmental analysis model, unless stated otherwise. The tissue-to-blood C_{max} and AUC_{last} (area under the curve until last time point) ratios were calculated where possible. The AUC_{last} ratios were calculated using the linear trapezoidal rule.

Results

Blood/Plasma Pharmacokinetics. After intravenous administration of [^{3}H]-SSB siRNA in LNP vehicle, the concentrations of radiolabeled components were measurable throughout the observation periods in blood and plasma (504 hours p.d.; Fig. 1). The concentration of total radiolabeled components declined in a multiexponential manner in both matrices. Following the apparent C_{max} at 5 and 60 minutes, the radioactivity declined to 72 hours post dose, and a slower decline occurred from 72 hours post dose onward for dried blood and plasma, respectively. The apparent terminal elimination half-life of blood was 162 hours. Samples dried prior to radioactivity analysis showed, in all cases, lower levels of total radioactivity, suggesting the formation of tritiated water. Measurements of dried blood were comparable with results derived from QWBA data, as shown in Fig. 2.

Pharmacokinetics of the Guide Strand of [^{3}H]-SSB siRNA (LC-MS-RA). The parent guide strand of [^{3}H]-SSB siRNA was detectable up to 48 hours after dosing in plasma by LC-MS-RA, as depicted in Fig. 1. Pharmacokinetic parameters are presented in Table 1. Radiochromatogram profiles are presented in Fig. 3. Following the apparent C_{max} at 1 hour (1.04 μM equivalents), an elimination phase was identified, with an observed decline until 48 hours.

Pharmacokinetics of the Guide and Passenger Strands of SSB siRNA (RT-qPCR). The parent guide and passenger strands of SSB siRNA were measured in plasma after intravenous administration of radioactive and nonradioactive SSB siRNA in LNP vehicle, by means of RT-qPCR, as shown in Fig. 1. Pharmacokinetic parameters are presented in Table 1. Concentrations of the guide and passenger strands were measurable up to 168 and 72 hours post dose, respectively. C_{max} values were observed at 60 and 5 minutes after dosing with an average value of 2.56 and 0.79 μM equivalents for guide and passenger strands, respectively. Following the apparent C_{max} for both strands, elimination phases were identified with an observed decline until 72 hours. For the guide strand, a clear slower elimination phase was observed from 72 to 168 hours. Determination of the guide strand was conducted by two methods (RT-qPCR and LC-MS-RA), and they correlated well, as shown in Fig. 1. AUC infinity (AUC∞) was approximately 1.2-fold greater than LC-MS-RA when determined by RT-qPCR. The AUC∞ ratios of guide strand and total radiolabeled components were 0.33 and 0.29 when determined by RT-qPCR and LC-MS-RA, respectively. This indicated that siRNA degradation products were the predominant component of total radioactivity in dried plasma.

Pharmacokinetics of the Cationic Lipid in the LNP Vehicle (LC-MS). The cationic lipid DLin-KC2-DMA in the LNP vehicle was determined in plasma by LC-MS, and concentrations were measurable up to 672 hours after dosing, as depicted in Fig. 1; pharmacokinetic parameters are in Table 1. The peak value of concentration (C_{max}) was observed at 5 minutes post dose, with an average value of 685 μM equivalents. Following the apparent C_{max}, a decline from 5 minutes to 72 hours post dose (phase 1) was followed by a slower decline with an apparent terminal elimination half-life of 198 hours.

Tissue Distribution of Total Radiolabeled Components Determined by QWBA. Following a single intravenous administration of [^{3}H]-SSB siRNA in LNP vehicle, radioactivity was detected in all tissues investigated. The time where the maximum concentration (T_{max}) was observed at 1 hour p.d. in most tissues/matrices, and the highest concentrations of total radiolabeled components (C_{max}) and exposure (AUC_{last}) were observed in spleen (red pulp), liver, esophagus, and nonglandular stomach, which were 1.0- to 3.0-fold and 2.7- to 4.8-fold higher than in blood (0.52 μM equivalents), respectively. At 168 hours, radioactivity was quantifiable in most tissues/matrices, with concentrations higher than in blood (with the exception of four tissues). Figure 2 displays concentration-time profiles of total radiolabeled components in dried blood, plasma, and selected tissues, and Fig. 4 displays selected whole-body autoradioluminograms at 1, 48, and 168 hours p.d.

Tissue Distribution of Cationic Lipid Determined by MALDI-MS Imaging. The sensitivity of MS imaging allowed specific detection of cationic lipid DLin-KC2-DMA in sections from all time

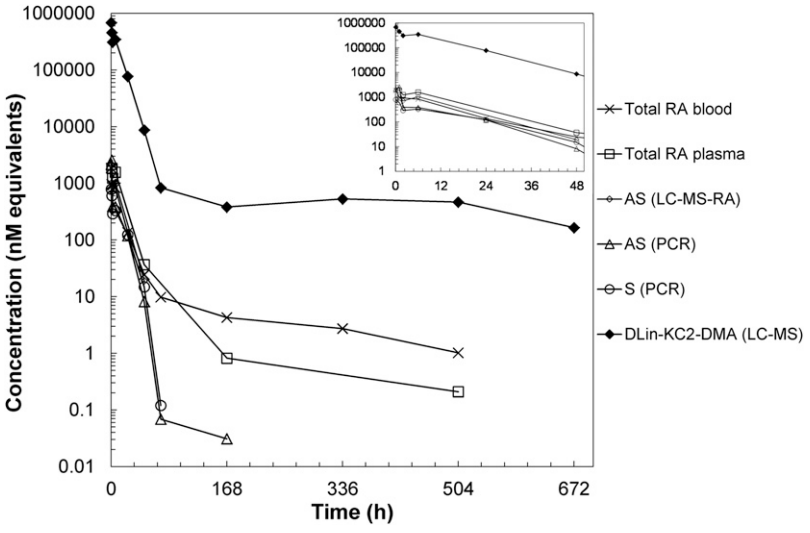

Fig. 1. Concentrations of guide (AS, determined by both RT-qPCR and LC-MS-RA) and passenger strand (S, determined by RT-qPCR) of SSB siRNA, cationic lipid DLin-KC2-DMA (one of the main excipients of the LNP vehicle, determined by LC-MS), and total radiolabeled components in dried blood and plasma, after a single intravenous administration of [^{3}H]-SSB siRNA in LNP vehicle to CD-1 mice at 2.5 mg/kg. N = 1/time point.

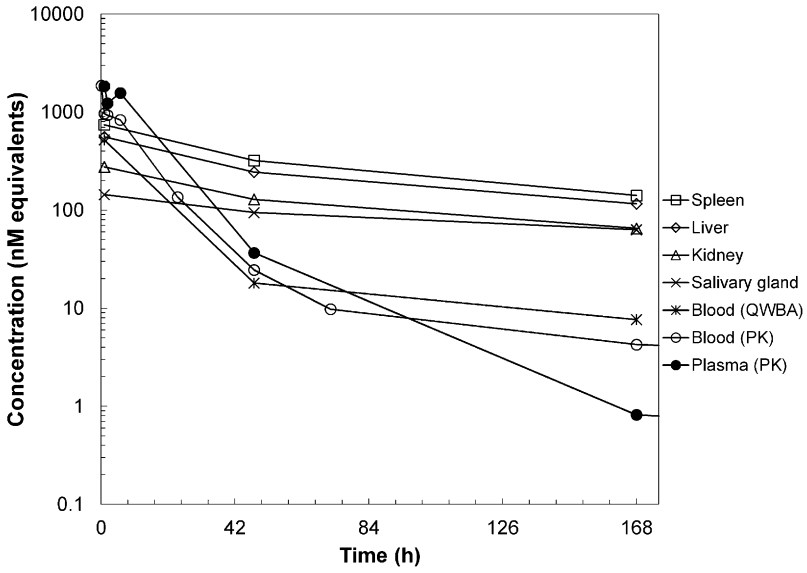

Fig. 2. Concentrations of total radiolabeled components in dried blood, plasma, and selected tissues after a single intravenous administration of [^{3}H]-SSB siRNA in LNP vehicle to CD-1 mice at 2.5 mg/kg. N = 1/time point.

points, with the highest observed concentrations in the liver and stomach. Figure 5 displays selected whole-body MALDI-MS images at 1, 48, and 168 hours post dosing. A semiquantitative assessment shows the highest tissue concentrations at 1 hour post dose. No lipid was found in brain tissue.

Metabolic Stability of ^{3}H Label. The fraction of the administered radioactive dose converted to tritiated water was initially estimated using urine and blood as matrices, as previously reported (Christensen et al., 2013). Concentration-time course of tritiated water in body water resulted in apparent elimination half-life values of 108 and 115 hours in urine and blood, respectively (Supplemental Fig. 1). These values did not correlate with the expected (27.1 hours) apparent elimination half-life value of water in mice (Richmond et al., 1962). Therefore, the formation rate constants of tritiated water were estimated as 77 and 73 hours in urine and blood, respectively. Assuming a first-order rate of formation, and an elimination rate for tritiated water of 27.1 hours, curve fitting was performed (Supplemental Fig. 2). These modulated results indicated that the formation of tritiated water was the rate-limiting step, and not the elimination.

Considering the estimated formation rate constant of tritiated water, the total amount of tritiated water was estimated with the following assumptions: 1) the elimination half-life (T1/2) of water in the mouse was 27.1 hours (Richmond et al., 1962); 2) the volume of distribution of tritiated water was equal to the body water (72.5% of body weight) (Davies and Morris, 1993); 3) the concentration-time courses of tritiated water were derived from urine and blood; And 4) the amount formed was estimated by using the deconvolution method given in Phoenix WinNonlin software (version 6.1.0.173; Pharsight Corp.).

Following intravenous administration, the percentage of administered radioactivity transformed to tritiated water tended to increase with time in mice. Eighty percent and 105% of the dose was estimated to be transformed into tritiated water at 504 hours after dosing in urine and blood, respectively (Supplemental Fig. 3). This increase indicated that the formation of tritiated water was an ongoing process, and an average value considering all urine and/or blood sample time points could not be given. Therefore, the urine values derived from 48, 168, and 504 hours were used for the mass balance calculation, since these values reflected the total formation of tritiated water most accurately.

Mass Balance (Excretion). Mass balance data obtained at 48, 168, and 504 hours p.d. are presented in Table 2. Up to 48, 168, and 504 hours after administration, tritiated water was estimated to be formed by 18%, 53%, and 80% of the radioactive dose, respectively. Tritiated water was formed with a slow formation rate. The reason of the high amount of tritiated water formed was ascribed to the relatively long retention period of total radiolabeled compounds in the body (this could also be caused by the endogenous metabolism of uridine nucleosides; however, ongoing research suggests this is not the case). The weak overall recovery determined in the samples was ascribed to

TABLE 1

Blood/plasma pharmacokinetic parameters estimated for radiolabeled components, parent compound, and cationic lipid after a single i.v. administration of LNP-formulated [^{3}H]-SSB siRNA

Parameter	Radiolabeled Components		Parent Guide (AS) or Passenger (S) Strand of SSB siRNA			Cationic Lipid
	Blood (Dried)	Plasma (Dried)	Plasma AS[a] (LC-MS-RA)	Plasma AS[a] (qPCR)	Plasma S[a] (qPCR)	Plasma (LC-MS)
Actual dose (mg/kg)	2.51	2.51	2.51	2.54	2.54	10.6
C_{max} (μM equivalents)	1.92	1.90	1.04	2.56	0.79	685
AUC_{last} (h $\times$ μM equivalents)	19.2	47.2	13.5	13.8	7.01	NA
AUC∞ (h $\times$ μM equivalents)	19.5	47.2	13.7	15.8	7.01	6587
T1/2 (h)	162	NA	NA	NA	NA	198
Cl (mL / (h $\times$ kg))	NA	NA	13.6	11.9	26.9	0.1
V (mL / kg)	NA	NA	NA	NA	247	34

CL, clearance; NA, not applicable; T1/2, half-life; V, volume of distribution.
[a]Analyzed by a two-compartment model.

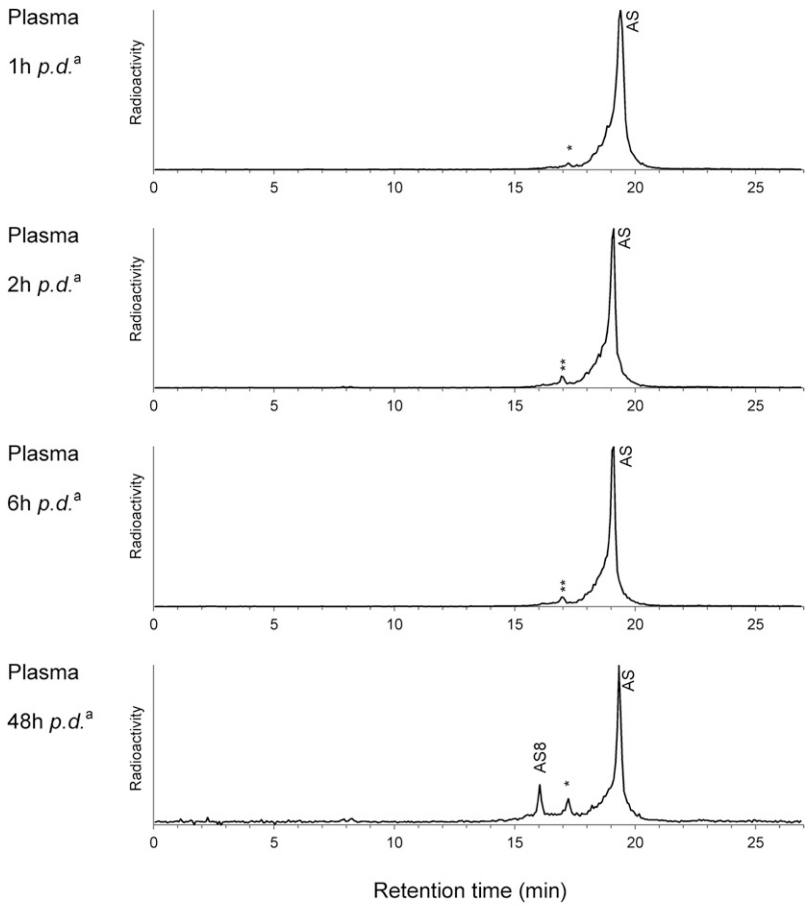

a) Proposed metabolites: *AS3/AS4/AS6/AS8P/AS7; **AS7/AS9P/AS9.

Fig. 3. Metabolite profiles of LNP-formulated [^{3}H]-SSB siRNA in plasma following a single i.v. administration (nominal dose 2.5 mg/kg, analysis of SPE elution fractions).

loss of tritiated water by evaporation. Renal elimination was the main route of excretion. Overall, the recovery was 93% (including the estimated tritiated water, excreta, and carcass).

Determination of Free Radioactivity by Gel Electrophoresis and Radiometry. The LNP formulation protects the siRNA from rapid in vivo degradation, which leaves the free siRNA (nonencapsulated) as the only source of material to be metabolized. If the amount of free material is low, metabolite profiling will be challenging. Therefore, the free radioactivity was first determined. The free radioactivity, assumed to represent metabolites, is the radioactivity that is not associated with the LNP vehicle.

Method development and validation was as follows. Agarose gel electrophoresis was chosen over PAGE due to its higher dissolution property. The method was tested in blood and plasma, and in PBS as a control. The distribution of radioactivity in the lane sections of blood and plasma correlated well with the PBS control (Supplemental Table 1). No matrix effect was observed, supporting its application for both plasma and blood samples. The method was validated by testing the dosing solution of the LNP-formulated [^{3}H]-SSB siRNA in plasma (in duplicate). For control, triton was added to an aliquot to disrupt the LNP formulation. The degree of encapsulation of [^{3}H]-SSB/LNP in plasma was determined to be 91% (mean of two runs) by the agarose gel electrophoresis and radiometry method (Supplemental Table 1). This was in line with the results obtained by SEC-HPLC after LNP formulation (88.3%). The control samples containing triton disrupted the LNP formulation as expected, but not completely (9% left in the well).

Selected radioactive plasma samples (1, 6, 48, and 504 hours) were analyzed, and the results are presented in Supplemental Table 2. In all investigated plasma samples, high percentages of radioactivity were found in the well, supporting the conclusion that the radioactivity in the central circulation is mainly associated with formulated material. However, detectable amounts of radioactivity up to 30% of total radioactivity per sample were measured in the middle and end of the gel, suggesting that nonformulated material is present in the plasma. The control samples, containing triton, disrupted the LNP formulation as expected, though not completely, especially for the 48-hour p.d. (54% left in the well). A possible cause for this could be explained by insufficient mixing before loading. With the amounts of nonformulated material being reasonably available, metabolite profiling was initiated.

Metabolite Profiles in Plasma. The radioactive plasma samples up to 504 hours post dosing were prepared for LC-MS-RA analysis by SPE, and the distribution of radioactivity in the solid phase extraction (SPE) fractions, at the early time points, indicated a low turnover of the parent guide strand (data not shown). The SPE wash fractions contained only a minor fraction of the radioactivity (0%–2%), which indicated that the radiolabeled nucleosides were not a major component in plasma (the radioactive monomer was known, if present, to elute in the SPE wash fraction). Furthermore, the fraction of radioactivity observed in the SPE load fractions increased over time, which indicated that high amounts of tritiated water were formed over time. These results are in line with the estimations of the formation of tritiated water in blood.

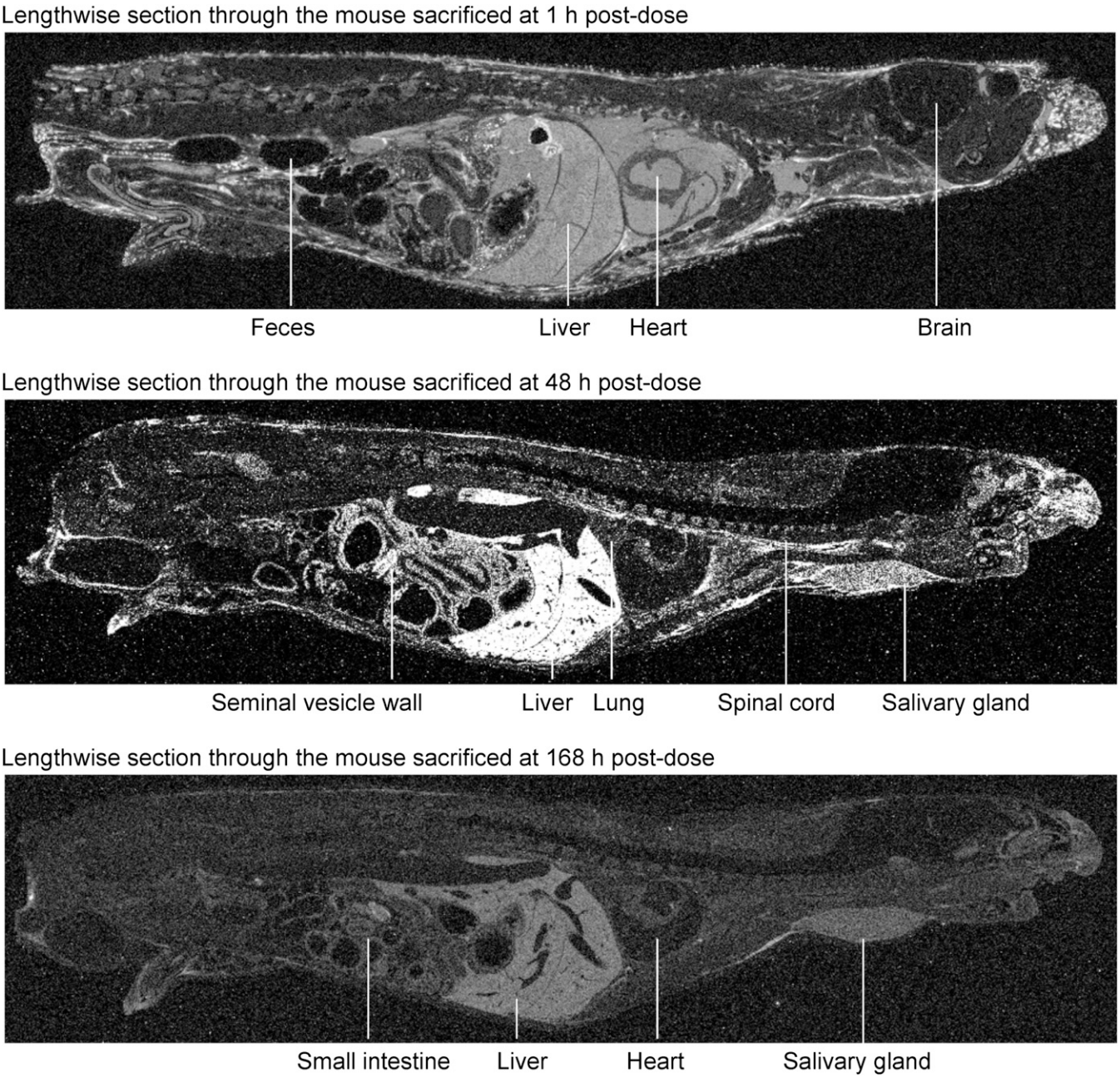

Fig. 4. Selected whole-body autoradioluminographs at 1, 48, and 168 hours after a single intravenous administration of [^{3}H]-SBB siRNA in LNP vehicle (nominal dose: 2.5 mg/kg) to male CD-1 mice. The whitest area corresponds to the highest concentration of radiolabeled components.

Metabolite profiles in plasma were assessed up to 48 hours after dosing, and the profiles are shown in Fig. 3. Intact guide strand (AS) was observed up to 48 hours post dosing in plasma, as depicted in Fig. 1. 14-18Mer oligonucleotide metabolites were identified by a corresponding peak in the radiochromatogram versus a control sample, and have to be considered as proposals only. Consult Christensen et al. (2013) (incl. Table S4 Supplemental Data) for metabolite nomenclature, assignment, structural elucidation, and identification.

Discussion

This study presents the ADME properties of an siRNA formulated in an LNP vehicle, after intravenous administration in mice. The siRNA, SSB, targets the ubiquitous gene Sjögren syndrome antigen B, and was 2´-O-methyl chemically modified. After injection of the LNP-formulated SSB siRNA, the parent guide strand of siRNA could be determined in plasma up to 48 and 168 hours p.d. by LC-MS-RA and RT-qPCR, respectively. Determination of the guide strand concentrations by these two techniques correlated well with each other. The half-life values were significantly longer than after i.v. administration of the unformulated [^{3}H]-SSB siRNA, as recently reported (Christensen et al., 2013), where 5-minute p.d. no parent guide strand was observed. The extended half-life of the siRNA observed with liposome formulations has also been reported by Morrissey et al. (2005), where formulation of the siRNA increased the circulation time to 6.5 hours, compared with the unformulated chemically stabilized version, which showed an elimination half-life of 0.8 hour.

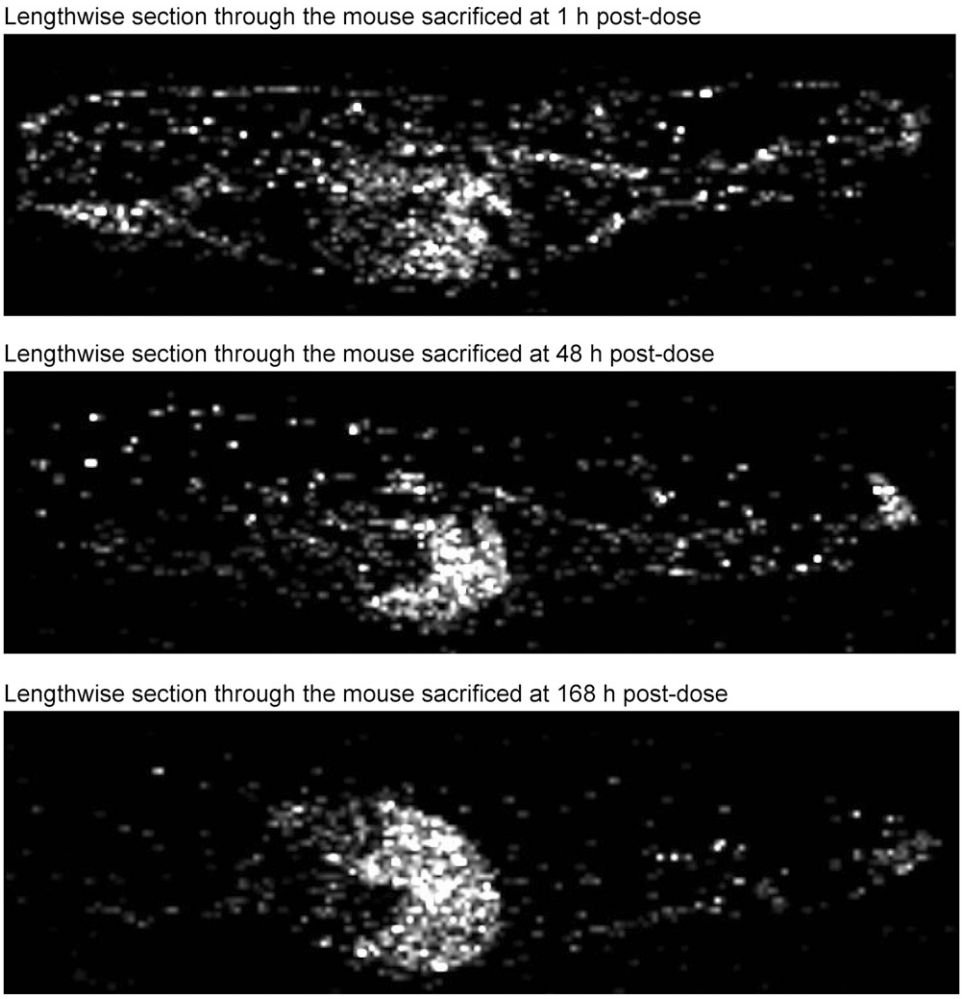

Fig. 5. Selected whole-body MALDI-MS images at 1, 48, and 168 hours after a single intravenous administration of [^{3}H]-SBB siRNA in LNP vehicle (nominal dose: 2.5 mg/kg) to male CD-1 mice. The whitest area corresponds to the highest concentration of DLin-KC2-DMA (one of the main excipients of the LNP vehicle).

The half-life of the passenger strand was also determined by RT-qPCR up to 72 hours p.d. The observed half-lives for the guide and passenger strands were similar, suggesting that the siRNA circulating in plasma was still in its intact duplex format. The lowest parent guide strand concentration detected by LC-MS-RA was 19 nM equivalents. The RT-qPCR technique was shown to be approximately 300 times more sensitive than the LC-MS-RA method. In general, the higher sensitivity obtained by PCR methods makes these approaches more attractive than LC-MS. However, PCR methods do not distinguish full-length oligonucleotides from metabolites formed via the truncation of one or more single nucleotides, which can result in an overestimation of the parent compound.

The AUC∞ calculated from RT-qPCR was approximately 1.2-fold greater than that calculated using LC-MS-RA. Nevertheless, the difference was not considered to be significant, and could also have been caused by analytical variation among the two techniques. In addition, PCR methods may not work for extensively chemically modified sequences, which could be a plausible explanation why the AUC∞ was approximately 2.3-fold greater for the guide strand than for the passenger strand (more modified) when determined by RT-qPCR.

TABLE 2

Mass balance: excretion and recovery of total radiolabeled components of male CD-1 mice following a single intravenous administration of [^{3}H]-SBB siRNA in LNP vehicle (nominal dose: 2.5 mg/kg)

Values are the percentage of dose.

[^{3}H]-SSB in LNP Vehicle	Urine	Feces	Carcass	Tritiated Water	Total
48 h	14	2	46	18	80
168 h	18	3	16	53	90
504 h	18	3	9	80	110

Separation of the metabolites by LC and subsequent identification by radiodetection and accurate mass spectrometry provides a powerful tool to elucidate the in vivo fate of siRNAs. The AUC∞ ratio of the guide strand and radiolabeled components indicated that siRNA degradation products were the predominant component of total radioactivity in (dried) plasma. 14-18Mer oligonucleotide metabolites were observed in plasma. Complete degradation of the guide strand to the radiolabeled nucleoside was not observed in this study using the LNP-formulated siRNA.

Our semiquantitative gel and radiometry method revealed that the majority of the total radioactivity in plasma was associated with the vehicle, increasing the likelihood of intact siRNA in circulation. This supports the hypothesis that the LNP formulation prohibits the siRNA from being metabolized. In addition, 14%–30% of the total radioactivity in selected plasma samples (1, 6, and 48 hours p.d.) was associated with free (nonencapsulated) radioactivity. From the radiochromatogram profiles (Fig. 3), 17%–30% of the total radioactivity was ascribed to metabolites (at 1, 6, and 48 hours p.d.). These results were in line with the data derived from the gel electrophoresis

and radiometry approach. This demonstrated that the method was applicable for determination of free versus encapsulated radioactivity in biosamples, and therefore assessing if metabolite profiling was of relevance.

The cationic lipid DLin-KC2-DMA in the LNP vehicle was also determined in plasma by LC-MS, and concentrations were measurable up to 672 hours after dosing. Following the apparent C_{max} values of total radiolabeled components, SSB siRNA, and DLin-KC2-DMA, the first elimination phase was relatively long (up to at least 72 hours). Long terminal half-life values of total radiolabeled components in both matrices (blood and plasma) and of DLin-KC2-DMA indicated a long residence time of radiolabeled SSB siRNA and/or metabolites in the body. It was concluded that the disposition of SBB siRNA was determined by the pharmacokinetics of the LNP vehicle (analyte DLin-KC2-DMA as surrogate).

After injection of the LNP-formulated [^{3}H]-SSB siRNA, the radioactivity was detected throughout the body, but in low concentrations compared with blood (maximum of up to 3-fold). The tissues with the highest concentrations and exposures of radioactivity were the spleen, liver, esophagus, and stomach. A week after dosing, the concentrations of radioactivity were generally higher in tissues than in blood. Measurements of (dried) blood were comparable with results derived from the blood pharmacokinetic data. Other biodistribution studies in mice have also reported the spleen and/or liver as the major organs of distribution of radioactivity after systemic administration of formulated siRNA (Bartlett et al., 2007; de Wolf et al., 2007; Sonoke et al., 2008; Malek et al., 2009; Merkel et al., 2009a; Mudd et al., 2010).

Concentration data alone do not give information about efficacy. Therefore, as highlighted in a recent PK/PD relationship study by Wei et al. (2011), high concentrations of siRNA at the desired target organ do not necessarily correlate with a high knock-down level of the desired mRNA. Factors that are also likely to be needed for successful RNAi are as follows: number of Ago2-siRNA complexes, turnover of the Ago2 complex, stability of the siRNA, target mRNA half-life, mRNA expression levels, cell division and turnover, or a combination thereof.

MALDI-MS imaging allowed the label-free detection of the cationic lipid, providing specific information on the delivery vehicle of the siRNA. Although MALDI-MS imaging also supports detection of siRNA, the tissue concentrations in this experiment were below the detection limit of this technique. By combining the data from QWBA and MALDI-MSI, one can obtain a complete result. The data showed that the observed distribution of the radiolabeled siRNA (followed by QWBA) correlated well with the distribution observed for the cationic lipid (followed by MALDI-MSI), suggesting the siRNA/cationic lipid was distributed as an LNP complex.

The overall weak mass balance data were associated with the loss of tritiated water by evaporation. By inclusion of the estimated tritiated water, the recovery was 80%–110%. The high amount of tritiated water formed was ascribed to the relatively long retention period of total radiolabeled compounds in the body. Recovery of radioactivity in excreta (especially urine) was significantly lower than when using unformulated [^{3}H]-SSB siRNA (38% in urine) (Christensen et al., 2013). Renal excretion remained the main route of excretion. At 48 and 168 hours after administration, 46% and 16% of the total radioactive dose, respectively, was still present in the carcass (tritiated water subtracted). These data were similar to the results derived from QWBA, where residual radioactivity after 48 and 168 hours was approximately 33% and 16% of the dose, respectively.

The observed renal excretion is in line with the reduced uptake of large molecules by the kidneys when using formulated siRNAs in nanoparticle carriers (Kawakami and Hashida, 2007). Nanoparticle carriers are rapidly distributed to organs in the reticuloendothelial system (RES) and phagocytosed by the mononuclear phagocyte system (e.g., macrophages and liver Kupffer cells). The function of RES is to clear the body of foreign pathogens, and of cells that have undergone apoptosis (Juliano et al., 2009). Liver and spleen are highly perfused organs which belong to the RES organs. The microvessels of both organs have relatively large fenestrations which allow entry of molecules up to approximately 200 nm (Huang et al., 2010; Wang et al., 2010b). Therefore, systemically delivered nanoparticles usually distribute in RES organs; the liver and spleen were among the organs with the highest distribution of radioactivity. Of note, the RES system also plays a role in the systemic delivery of unformulated siRNAs, particularly the liver (Juliano et al., 2009). Tumors are also amenable for the penetration of high molecular mass macromolecules (100–800 nm), due to the fact that they possess a leaky and discontinuous vasculature, a phenomenon known as enhanced permeation and retention effect (Wang et al., 2010a). Therefore, the particle size of the formulation used for systemic administration of siRNAs is important as it influences clearance rates, overall biodistribution, cellular uptake, and intracellular trafficking, and thus the final pharmacological outcome. The long terminal half-life of the LNP vehicle (analyte DLin-KC2-DMA as surrogate) in RES organs (liver and spleen) could be of concern, because in vivo toxicity often correlates with long-term deposition in RES organs (Juliano et al., 2009).

In conclusion, the LNP vehicle drove the kinetics and biodistribution of the SSB siRNA, and significantly reduced the renal clearance and increased its circulation time in plasma. We have demonstrated here that our previously described [^{3}H]-radiolabeling method of oligonucleotides is applicable for preclinical ADME studies of unformulated, as well as LNP-formulated, siRNAs. The [^{3}H]-labeled siRNAs have been proven to be both radio and chemically stable for at least 6 months at temperatures below −80°C. This should allow sufficient time to conduct any relevant in vivo studies. However, the labeling method has its limitations, as indicated by the increase in formation of tritiated water over time, particularly for the long-term study with the LNP-formulated [^{3}H]-siRNA (80% of the dose at 504 hours p.d.). Due to the formation of tritiated water, use of this type of labeling for human ADME studies is not recommended. To address this issue, placement of the tritium in the C6 position of a pyrimidine, instead of the current C5 position, could improve the metabolic stability, thereby reducing the formation of tritiated water. This could make the [^{3}H]-radiolabeling method more applicable to long-term ADME studies. Nevertheless, the [^{3}H]-radiolabeling method —in its current state—offers several advantages over existing oligonucleotide labeling techniques, where very few have appeared to be fully satisfactory with regard to choice of radioisotope, the position(s) of labeling (e.g., unstable positions, random labeling, end-labeling), and chemical modifications needed for coupling of the label. In these cases, it has to be assumed that their presence does not alter the reactivity or metabolism of the molecule. We have recently reported a head-to-head comparison of an ^{3}H- versus ^{111}In-labeled unformulated siRNA, and found that the ^{111}In-labeled siRNA (van de Water et al., 2006) showed different distribution and pharmacokinetics compared with the molecule labeled with ^{3}H (Christensen et al., 2013). Indeed, although binding kinetic in vitro could be similar, different distribution and kinetics were observed in vivo by introducing a significant modification to the structure of the siRNA. The methods presented here could be applied to a wide range of siRNA formulations and provide useful perspectives for the further development of in vivo applications of siRNA as therapeutics.

Acknowledgments

The authors thank Noah Gardner, Dr. Albrecht Glaenzel, and Patrick Bross for guidance and support with the LNP formulation of the [^{3}H]-siRNA. The authors would also like to acknowledge nonclinical PK/PD for their support with the animal and QWBA studies (Martina Suetterlin, Denise Schaerer, and Heidrun Reilmann). The authors would like to extend our thanks to Dr. Fred Asselbergs for PCR analysis, Gregory Morandi for MALDI-MS imaging analysis, and Samuel Barteau for LC-MS analysis of the cationic lipid.

Authorship Contributions

Participated in research design: Christensen, Litherland, Faller, van de Kerkhof, Natt, Hunziker, Krauser, Swart.

Conducted experiments: Christensen.

Contributed with new reagents or analytic tools: Faller, van de Kerkhof, Boos, Beuvink, Bowman, Baryza, Beverly, Vargeese, Heudi, Stoeckli, Swart.

Performed data analysis: Christensen, Litherland, Faller, van de Kerkhof, Boos, Beuvink, Bowman, Heudi, Stoeckli, Swart.

Wrote or contributed to the writing of the manuscript: Christensen, Litherland, Faller, van de Kerkhof, Krauser, Swart.

References

Bartlett DW, Su H, Hildebrandt IJ, Weber WA, and Davis ME (2007) Impact of tumor-specific targeting on the biodistribution and efficacy of siRNA nanoparticles measured by multimodality in vivo imaging. *Proc Natl Acad Sci USA* **104**:15549–15554.

Behlke MA (2008) Chemical modification of siRNAs for in vivo use. *Oligonucleotides* **18**: 305–319.

Boos JA, Kirk DW, Piccolotto ML, Zuercher W, Gfeller S, Neuner P, Dattler A, Wishart WL, Von Arx F, and Beverly M, et al. (2013) Whole-body scanning PCR; a highly sensitive method to study the biodistribution of mRNAs, noncoding RNAs and therapeutic oligonucleotides. *Nucleic Acids Res* **41**:e145.

Burnett JC, Rossi JJ, and Tiemann K (2011) Current progress of siRNA/shRNA therapeutics in clinical trials. *Biotechnol J* **6**:1130–1146.

Christensen J, Litherland K, Faller T, van de Kerkhof E, Natt F, Hunziker J, Krauser J, and Swart P (2013) Metabolism studies of unformulated internally [3H]-labeled short interfering RNAs in mice. *Drug Metab Dispos* **41**:1211–1219.

Christensen J, Natt F, Hunziker J, Krauser J, and Swart P (2012) Tritium labeling of full-length small interfering RNAs. *J Labelled Comp Radiopharm* **55**:189–196.

Davies B and Morris T (1993) Physiological parameters in laboratory animals and humans. *Pharm Res* **10**:1093–1095.

de Wolf HK, Snel CJ, Verbaan FJ, Schiffelers RM, Hennink WE, and Storm G (2007) Effect of cationic carriers on the pharmacokinetics and tumor localization of nucleic acids after intravenous administration. *Int J Pharm* **331**:167–175.

Gao S, Dagnaes-Hansen F, Nielsen EJB, Wengel J, Besenbacher F, Howard KA, and Kjems J (2009) The effect of chemical modification and nanoparticle formulation on stability and biodistribution of siRNA in mice. *Mol Ther* **17**:1225–1233.

Hatanaka K, Asai T, Koide H, Kenjo E, Tsuzuku T, Harada N, Tsukada H, and Oku N (2010) Development of double-stranded siRNA labeling method using positron emitter and its in vivo trafficking analyzed by positron emission tomography. *Bioconjug Chem* **21**:756–763.

Huang L, Sullenger B, and Juliano R (2010) The role of carrier size in the pharmacodynamics of antisense and siRNA oligonucleotides. *J Drug Target* **18**:567–574.

Juliano R, Bauman J, Kang H, and Ming X (2009) Biological barriers to therapy with antisense and siRNA oligonucleotides. *Mol Pharm* **6**:686–695.

Kawakami S and Hashida M (2007) Targeted delivery systems of small interfering RNA by systemic administration. *Drug Metab Pharmacokinet* **22**:142–151.

Malek A, Merkel O, Fink L, Czubayko F, Kissel T, and Aigner A (2009) In vivo pharmacokinetics, tissue distribution and underlying mechanisms of various PEI(-PEG)/siRNA complexes. *Toxicol Appl Pharmacol* **236**:97–108.

Merkel OM, Librizzi D, Pfestroff A, Schurrat T, Béhé M, and Kissel T (2009a) In vivo SPECT and real-time gamma camera imaging of biodistribution and pharmacokinetics of siRNA delivery using an optimized radiolabeling and purification procedure. *Bioconjug Chem* **20**:174–182.

Merkel OM, Librizzi D, Pfestroff A, Schurrat T, Buyens K, Sanders NN, De Smedt SC, Béhé M, and Kissel T (2009b) Stability of siRNA polyplexes from poly(ethylenimine) and poly (ethylenimine)-g-poly(ethylene glycol) under in vivo conditions: effects on pharmacokinetics and biodistribution measured by Fluorescence Fluctuation Spectroscopy and Single Photon Emission Computed Tomography (SPECT) imaging. *J Control Release* **138**:148–159.

Morrissey DV, Lockridge JA, Shaw L, Blanchard K, Jensen K, Breen W, Hartsough K, Machemer L, Radka S, and Jadhav V, et al. (2005) Potent and persistent in vivo anti-HBV activity of chemically modified siRNAs. *Nat Biotechnol* **23**:1002–1007.

Mudd SR, Trubetskoy VS, Blokhin AV, Weichert JP, and Wolff JA (2010) Hybrid PET/CT for noninvasive pharmacokinetic evaluation of dynamic PolyConjugates, a synthetic siRNA delivery system. *Bioconjug Chem* **21**:1183–1189.

Rettig GR and Behlke MA (2012) Progress toward in vivo use of siRNAs-II. *Mol Ther* **20**: 483–512.

Richmond CR, Langham WH, and Trujillo TT (1962) Comparative metabolism of tritiated water by mammals. *J Cell Comp Physiol* **59**:45–53.

Semple SC, Akinc A, Chen JX, Sandhu AP, Mui BL, Cho CK, Sah DWY, Stebbing D, Crosley EJ, and Yaworski E, et al. (2010) Rational design of cationic lipids for siRNA delivery. *Nat Biotechnol* **28**:172–176.

Sonoke S, Ueda T, Fujiwara K, Sato Y, Takagaki K, Hirabayashi K, Ohgi T, and Yano J (2008) Tumor regression in mice by delivery of Bcl-2 small interfering RNA with pegylated cationic liposomes. *Cancer Res* **68**:8843–8851.

Van de Water FM, Boerman OC, Wouterse AC, Peters JGP, Russel FGM, and Masereeuw R (2006) Intravenously administered short interfering RNA accumulates in the kidney and selectively suppresses gene function in renal proximal tubules. *Drug Metab Dispos* **34**:1393–1397.

Wang Y, Li ZG, Han Y, Liang LH, and Ji AM (2010b) Nanoparticle-based delivery system for application of siRNA in vivo. *Curr Drug Metab* **11**:182–196.

Wang J, Lu Z, Wientjes MG, and Au JL (2010a) Delivery of siRNA therapeutics: barriers and carriers. *AAPS J* **12**:492–503.

Wei J, Jones J, Kang J, Card A, Krimm M, Hancock P, Pei Y, Ason B, Payson E, and Dubinina N, et al. (2011) RNA-induced silencing complex-bound small interfering RNA is a determinant of RNA interference-mediated gene silencing in mice. *Mol Pharmacol* **79**:953–963.

Address correspondence to: Dr. Karine Litherland, Novartis Pharma AG, Novartis Institutes for Biomedical Research, Drug Metabolism and Pharmacokinetics, Fabrikstrasse 14, 1.02, CH-4002 Basel, Switzerland. E-mail: karine.litherland@novartis.com